# Numerical Movable Bed Channels Required for Investigation of Various Sizes and Shapes Particle Motions in Gravel Bed Rivers

Tomoo Fukuda[1] and Shoji Fukuoka[2]

[1]Research and Development Initiative, Chuo University
Kasuga 1-13-27, Bunkyo-ku, Tokyo 112-8551, JAPAN
t-fukuda@tamacc.chuo-u.ac.jp

[2]Research and Development Initiative, Chuo University
Kasuga 1-13-27, Bunkyo-ku, Tokyo 112-8551, JAPAN
sfuku@tamacc.chuo-u.ac.jp

## 1. INTRODUCTION

Sorting of particles and imbrication on the bed surface with particles of large variety of sizes and shapes are seen in gravel-bed rivers and the mechanism of sediment transport is more complicated than that in sand-gravel bed rivers. To discuss the mechanism of gravel particle motions in streams, the Lagrangian numerical approaches are important because motions of the flow and particles near the bed surface during floods can be hardly measured in rapid flows. Most numerical studies in the Lagrangian method have used spheres and been carried out in short channels (dozens of times the particle size) applying the periodic boundary conditions. These approaches have not demonstrated important mechanisms of particle motions of various shapes and development mechanisms of the bed structures such as sortings of particles and bed waves. We developed a numerical movable bed channel capable of simulating three-dimensional motions of flow and particles of various sizes and shapes [1]. Irregular shape particles were made by the combination of several small spheres (as shown in Figure 1). This paper demonstrates the numerical movable bed channels required for investigations of flow and particle motions in gravel bed rivers with particles of various sizes and shapes and presents the results of the numerical movable bed experiments.

## 2. NUMERICAL METHOD

### 2.1 Numerical method of fluid motions

Fluid motions are simulated with the governing equations of the solid-liquid multiphase flow where the regions of gravel particles are considered as a different density fluid [2]. We applied the Smagorinsky model as the sub grid turbulence model:

$$\frac{\partial u_i}{\partial x_i}=0 \tag{1}$$

$$\frac{\partial u_i}{\partial t}+u_j\frac{\partial u_i}{\partial x_j}=g_i-\frac{1}{\rho}\frac{\partial P}{\partial x_i}+\frac{\partial}{\partial x_j}\left\{2(\nu+\nu_t)S_{ij}\right\} \tag{2}$$

$$\nu_t=(C_S\Delta)^2\sqrt{2S_{ij}S_{ij}} \tag{3}$$

where $u_i$ : $i$-direction averaged velocity including gravel particle regions in a fluid calculation cell, $\rho$: density, $P$: sum of pressure and isotropic component

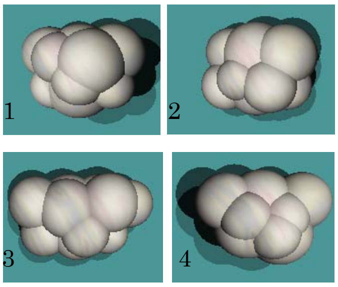

Figure 1. Different shapes of particles.

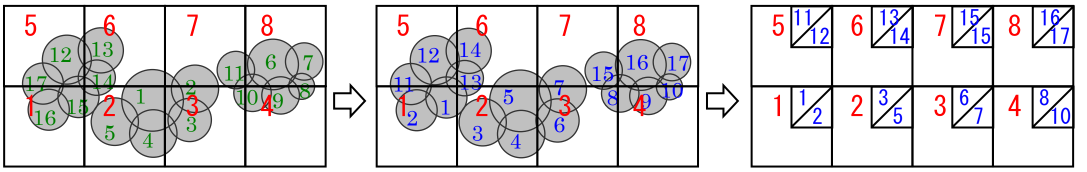

(a) Connecting cells numbers with sphere numbers

(b) Spheres sorted by cells number

(c) Maximum and minimum sorted sphere number in each cell

Figure 2 Relationship between cell number and sphere number.

of SGS stress, $g$: gravitational acceleration, $S_{ij}$: strain rate tensor, $\nu$: kinematic viscosity, $\nu_t$: SGS turbulent viscosity, $Cs$: Smagorinsky constant, $\Delta$: calculation grid size. Physical property (density $\rho$, dynamic viscosity $\mu$) and averaged velocity $u_i$ are calculated as volume-averaged values and mass-averaged values, respectively. Fluid forces acting on a particle are estimated with integrating forces acting on a particle region in the multiphase flow. Water surface variations are estimated by calculating advection of water volume fraction in fluid calculation cells with the Donor Cell Method.

## 2.2 Modeling of particles of various sizes and shapes

Particles of various sizes and shapes are made by the superposition of several small spheres as shown in Figure 1. The motion of gravel particles is simulated with the momentum equations and the angular momentum equations of rigid bodies. Rigid body properties of gravel particles (mass, gravity center and tensor of momentum inertia) are calculated by numerical integrations in consideration of positions and volumes of sufficiently small cells ($1.0\times10^{-9}$m$^3$) included in spheres composing gravel particles. Gravel particles refer to small spheres composing them and spheres do to gravel particles in this simulation, respectively. Gravel particles store small spheres composing them with Table 1(a) by MAXNSCG (the maximum number of spheres composing a gravel particle) and sphere numbers corresponding to each NSCG (number of spheres composing a gravel particle). Small spheres store the gravel particle number composing themselves with Table 1(b).

Table 1 Connecting gravel particle number with sphere number.

(a) List for gravel particles referring to sphere number.

| Gravel Particle No. | MAX NSCG | NSCG | Sphere No. |
|---|---|---|---|
| 1 | 5 | 1 | 1 |
| | | 2 | 2 |
| | | 3 | 3 |
| | | 4 | 4 |
| | | 5 | 5 |
| 2 | 6 | 1 | 6 |
| | | 2 | 7 |
| | | 3 | 8 |
| | | 4 | 9 |
| | | 5 | 10 |
| | | 6 | 11 |

⋮

(b) List for spheres referring to gravel number.

| Sphere No. | Gravel Particle No. |
|---|---|
| 1 | 1 |
| 2 | 1 |
| 3 | 1 |
| 4 | 1 |
| 5 | 1 |
| 6 | 2 |
| 7 | 2 |
| 8 | 2 |
| 9 | 2 |
| 10 | 2 |
| 11 | 2 |

⋮

Table 2 Relationship between sorted number and sphere number.

| Sorted No. | Sphere No. |
|---|---|
| 1 | 15 |
| 2 | 16 |
| 3 | 5 |

⋮

Table 3 List of contact candidate pair spheres.

| List No. (a) | Pair list (A)Smaller Sphere No. (b) | Pair list (B)Larger Sphere No. (c) | Forces acting on sphere A (d) | Contact Point (e) |
|---|---|---|---|---|
| 1 | 5 | 15 | $\boldsymbol{F}_1$ | $\boldsymbol{X}_1$ |
| 2 | 2 | 11 | $\boldsymbol{F}_2$ | $\boldsymbol{X}_2$ |

⋮

Table 4 Relationship between sphere number and list number.

| Sphere No. | List No. | | |
|---|---|---|---|
| 1 | | | |
| 2 | 2 | | |
| ⋮ | | | |
| 5 | 1 | | |
| ⋮ | | | |
| 11 | | | 2 |
| ⋮ | | | |
| 15 | | | 1 |
| ⋮ | | | |

## 2.3 Data flow in calculation of contact forces

The contact force and the motion of large numbers of particles in the numerical movable bed have to be calculated with the high speed. Nishiura and Sakaguchi [3] have developed the efficient algorithms of calculations of contact forces and motions of spheres on shared memory systems. We applied the PGS method (Contact candidate Paring of Grid based Sorted particle index) and the FSC method (Force Simulation referencing the Contact pair table) developed by Nishiura and Sakaguchi to the motions of gravel particles of various sizes and shapes. The general method for detections of spheres' contacts stores spheres into the near cells. It is, however, difficult to estimate maximum numbers of spheres to be in a cell before the simulation in the case of spheres of various sizes (shown in Figure 2(a)). This makes the determination of array size of cells for storing spheres difficult. The PGS method sorts the sphere number by the cell number shown in Fig 2 and Table 2. This makes it possible to store all spheres in the cells by storing the minimum sphere number and the maximum sphere number of spheres to be in the cell after the sorting. Therefore, the PGS method is effective for contact detection of spheres of various sizes in the numerical movable bed channel. Each sphere searches neighboring cells with Table 2 and makes the list of contact candidate pairs (Table 3 (a),(b),(c)) and Table 4 connecting the sphere number with the number of the list of contact candidate pairs (Table3). Each sphere refers to Table 1(b) and does not add overlapping spheres composing same gravel particles to the list of contact candidate pairs (Table 3). The FSC method calculates the contact forces $\boldsymbol{F}_n$ of contacting two spheres by referring to the list of contact candidate pairs (Table 3). To calculate torques acting on gravel particles of various sizes and shapes, we store contact points $\boldsymbol{X}_n$ with the Table 3. In the calculation of total contact forces $\boldsymbol{F}_g$ and torques $\boldsymbol{T}_g$ acting on a gravel particle, the gravel particle call spheres composing the gravel particles by referring to Table 1(a). The spheres refer to the contact pair list Table 3 by using Table 4 and calculate torques $\boldsymbol{T}_n$ by using contact forces $\boldsymbol{F}_n$ and contact points $\boldsymbol{X}_n$ stored in Table 3 and the gravity center of the gravel particle. Then the contact forces $\boldsymbol{F}_n$ and torques $\boldsymbol{T}_n$ are added to the forces $\boldsymbol{F}_g$ and torques $\boldsymbol{T}_g$ acting on the gravel particles. The routine summing up forces and torques of gravel particles is conducted with the loop of the gravel particle number in Table 1(a) and is able to be parallelized on a shared memory system without data conflict.

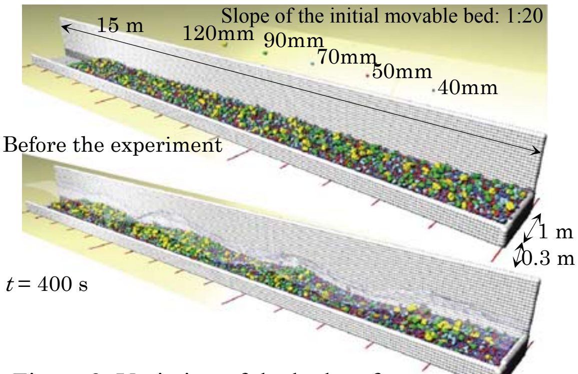

Figure 3. Variation of the bed surface.

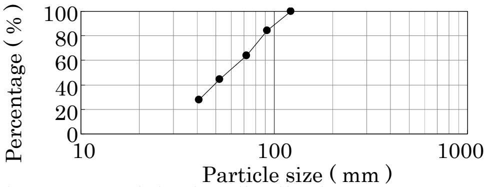

Figure 4. Particle size distributions.

## 3. NUMERICAL MOVABLE BED EXPERIMENT

Figure 3 shows the numerical movable bed channel. 20 types of particles (5 in sizes (40 mm, 50 mm, 70 mm, 90 mm, 120 mm) × 4 in shapes shown in Figure 1) were packed randomly in the channel of 15m long so that particle size distributions in the numerical channel agreed with the particle size distributions in Figure 4. The discharge of $0.5 \mathrm{m}^3/\mathrm{s}$ is given at the upstream end. The numerical experiment was lasted for 400 s. This numerical movable bed experiment was carried out by 33,470 gravel particles, 301,231 spheres composing gravel particles and 24,319,980 fluid calculation cells ($\Delta x = \Delta y = \Delta z = 0.01$ m).

## 4. RESULTS OF THE NUMERICAL MOVABLE BED EXPERIMENT

Figure 3 shows movable bed surfaces before and after the experiment. Large particles formed clusters and particle sortings occurred on the bed surface. Large particle clusters made protruding sections on the bed surface. The strong relationship was found between the sorting on the bed surface and the bed topography. The water surface variation of super-critical flow was simulated stably by the relatively simple estimation method. The developed numerical movable bed channel provides sound explanations for the motion of particles of various sizes and shapes and antidune formations. Figure 5 shows sediment transport rate of every particle size calculated at the downstream end. Sediment transport rate of smaller particles were great in the field experiments conducted in a gravel bed river (The Joganji river in Japan ) [4]. However, the sediment transport rates of larger particles are greater in the present numerical movable bed channel. The difference seems to be caused by the following reasons: the first, smaller particles than 40 mm are not included in the numerical movable bed channel which are transported easily and have a role of rollers for the motion of larger particles, the second, the fluid calculation cell size (one fourth of the smallest particles size) is relatively large for simulating fluid motions around smaller particles. The present numerical movable bed experiment took about 3 months by the calculation using shared memory systems (64core: Intel Xeon E7-8837 (2.67GHz) 8core×8). It is too much computation time.

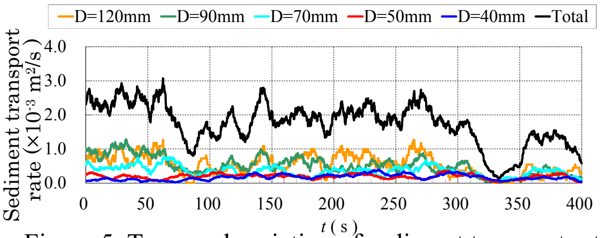

Figure 5. Temporal variation of sediment transport rate.

## 5. CONCLUSIONS

The present paper discussed results derived from the numerical movable bed channel experiments with particles of various sizes and shapes. Following main conclusions are obtained.

1)The numerical movable bed channel is able to simulate reasonably the motion of particles of various sizes and shapes, the sorting of particles at the bed surface and the motion of the flow on the bed waves.

2)The numerical channel with relatively large gravel particles showed that sediment transport rates of larger particles were greater than smaller particles. This seems not to be seen in the ordinary gravel bed rivers. The reason is because particles smaller than 40 mm are not included in the numerical channel and the fluid calculation cell size (one fourth of the smallest particles size) is larger for simulating fluid motions around small particles. The present numerical experiment took about three months. Large parallel computations on distributed memory systems are indispensable for higher performance of the computation with smaller particles and smaller fluid calculation cells.

References

[1] T. Fukuda, S. Fukuoka and T. Uchida: Three-dimensional motions in numerical movable bed channel with particles of various shapes and sizes, *12th International Symposium on River Sedimentation, Kyoto, Japan*.

[2] S. Ushijima, A. Fukutani and O. Makino: Prediction method for movements with collisions of arbitrary-shaped objects in 3D free-surface flows. *JSCE Journal* B 64(2), pp.128-138, 2008. in Japanese.

[3] D. Nishiura and H. Sakaguchi: Parallel-vector algorithms for particle simulations on shared-memory multiprocessors, *J. Computational physics*, No.230, pp.1923-1938. 2011.

[4] K. Soyama, Y. Ohkuma, Y. Hatanaka, F. Asano and S. Fukuoka: Study on observation technique and assessment of bed load discharge, *Advances in river engineering*, Vol. 17, pp.5-10, 2011, in Japanese.